IJISET - International Journal of Innovative Science, Engineering & Technology, Vol. 3 Issue 8, August 2016
ISSN (Online) 2348 – 7968 | Impact Factor (2015) - 4.332
www.ijiset.com

Effect of Zn Doping on Magnetic Properties of Magnesium Ferrite Nanoparticles

V. D. Murumkar

Department of Physics, Vivekanand Arts, Sardar Dalipsingh Commerce and Science College, Aurangabad

Abstract: Nanoparticles of zinc doped magnesium (Mg-Zn) spinel ferrite were prepared by using sol-gel auto combustion method. The prepared samples were characterized by X-ray diffraction technique and found single phase cubic spinel structure. The structural parameters as lattice constant, crystallite size and X-ray density were obtained from XRD data. The magnetic measurements as M-H of single phase nanocrystalline Mg-Zn spinel ferrite were carried out by pulse field hysteresis loop tracer technique at room temperature. The magnetic parameters like saturation magnetization, remanence magnetization and coercivity were obtained by M-H plots.

Keywords: Mg-Zn spinel ferrite, XRD, Crystallite size, Saturation magnetization

Introduction:

Spinel ferrites are commercially very important materials because of their excellent twin magnetic and electrical properties [1-3]. Recently the synthesis of magnetic nano particles has gained the considerable interest in material processing technologies and in the fabrication of novel materials. The $MgFe_2O_4$ spinel ferrite nanoparticles are important for its magnetic properties, particularly superparamagnetic behavior, which can be used for various applications. They exhibit interesting properties thus they can be used in different applications such as high density recording, high frequency devices, ferrofluids, new pigments, magnetic refrigerators etc [4-7]. $MgFe_2O_4$ has a well known cubic spinel structure in which the cations Mg^{2+} and Fe^{3+} are unequally distributed among the tetrahedral (A) and octahedral [B] sublattice sites. It has an inverse spinel structure [8, 9] while the $ZnFe_2O_4$ has normal spinel structure in which the Zn^{2+} cations reside on the tetrahedral site [10, 11]. Interestingly both the Zn^{2+} and Mg^{2+} are non-magnetic but still influence the structural and magnetic properties due to their different preferences on the lattice sites [12]. Mg-Zn ferrites are useful as core materials over a wide frequency range from few hundred hertz to several megahertz [13-15].
In the present investigation, the studies on structural and magnetic properties of nanocrystalline Mg-Zn spinel ferrite synthesized by using low temperature sol-gel auto-combustion technique are described.

Results and discussion:

X-Ray Diffraction:

The X-ray diffraction (XRD) patterns of $Mg_{1-x}Zn_xFe_2O_4$ (x = 0.00 and 0.30) recorded at room temperature in the 2θ range 20-80 degree are shown in figure 1.

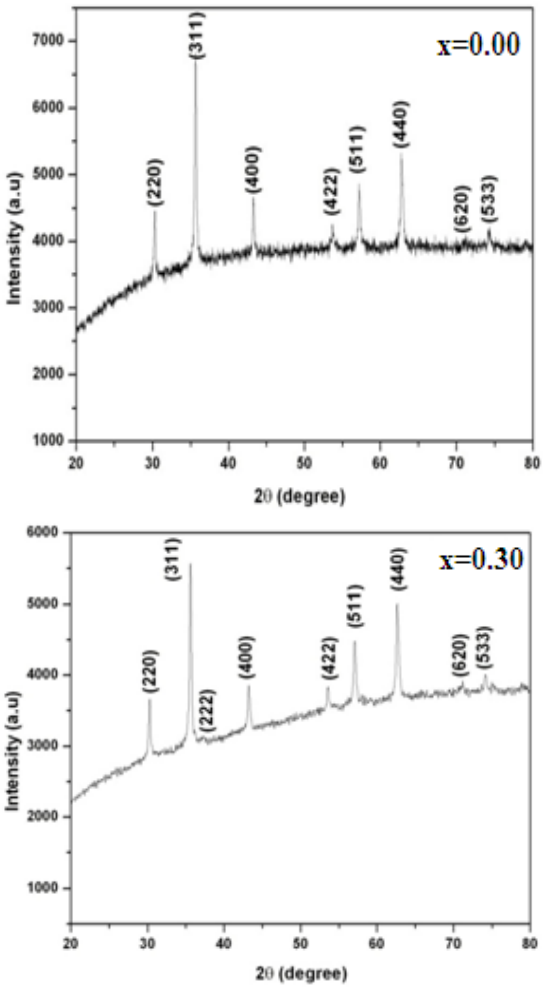

Figure 1: XRD patterns of $Mg_{1-x}Zn_xFe_2O_4$ (x = 0.00 and 0.30)

Table 1: Miller indices (h k l), Bragg's angle (2θ), Interplanar spacing (d), Intensity (I) and Relative intensity ratio (I/Io) of $Mg_{1-x}Zn_xFe_2O_4$(x = 0.00)

h k l	2θ (degree)	Sin (θ)	Sin θ/λ	d (Å)	I (a.u.)	I/I_O
(220)	30.30	0.26	0.169	2.9465	4471.8	65.4
(311)	35.65	0.30	0.1987	2.5158	6842.6	100.0
(400)	43.25	0.36	0.2392	2.0899	4666.5	68.2
(422)	53.67	0.45	0.2930	1.7062	4264.2	62.3
(511)	57.19	0.47	0.3107	1.6092	4877	71.3
(440)	62.75	0.52	0.3380	1.4794	5330.6	77.9
(620)	71.16	0.58	0.3777	1.3238	4112	60.1
(533)	74.29	0.60	0.3920	1.2755	4219.5	61.7

Table 2: Miller indices (h k l), Bragg's angle (2θ), Interplanar spacing (d), Intensity (I) and Relative intensity ratio (I/Io) of $Mg_{1-x}Zn_xFe_2O_4$ (x = 0.30)

h k l	2θ (degree)	Sin (θ)	Sin θ/λ	d (Å)	I (a.u.)	I/I_O
(220)	30.252	0.261	0.1694	2.9519	3690.3	65.4
(311)	35.598	0.306	0.1984	2.5199	5645.3	100.0
(222)	37.86	0.324	0.2106	2.3744	3906	69.2
(400)	43.242	0.368	0.2392	2.0905	3865.5	68.5
(422)	53.634	0.451	0.2928	1.7074	3894	69.0
(511)	57.088	0.478	0.3102	1.6120	4528.4	80.2
(440)	62.638	0.520	0.3374	1.4819	5045.7	89.4
(620)	70.963	0.580	0.3768	1.3271	3964.1	70.2
(533)	74.18	0.603	0.3915	1.2773	4049.1	71.7

XRD patterns show the sharp and intense peaks as (220), (311), (222), (400), (422), (511), (440), (620) and (533) which belongs to cubic phase spinel structure. Moreover there is no impurity peaks observed in the XRD patterns. This confirms the formation of single phase cubic spinel structure. The Miller indices, 2θ position, interplanar spacing, intensity and intensity ratio of each peak is given in table 1 and 2 for x=0.00 and x=0.30 respectively.

The most intense peak i.e. (311) was used to calculate the crystallite size of each sample using Scherrer's formula [16]. The lattice constant obtained using the relation $a=d\sqrt{h^2+k^2+l^2}$ where d is interplanar spacing and (hkl) are the Miller indices. The observed values of lattice constant are found to increase with zinc substitution which can be attributed to the larger ionic radius of the Zn^{2+} (0.82Å) than that of Mg^{2+} (0.78Å). The values of unit cell volume were obtained from the values of lattice constant. The X-ray density and bulk density of the samples were calculated using the standard relations [17]. The X-ray density increases with zinc substitution which is due to increase in molecular weight of the composition. Using the values of X-ray density and bulk density the porosity was calculated and found to be in the range of 17-19%. The values of lattice constant, crystallite size, unit cell volume, molecular weight, X-ray density, bulk density and porosity are tabulated in table 3. The obtained results are analogous to that of reported for Zn-Mg spinel ferrite [18].

Table 3: Lattice parameter (a), Volume (V), Molecular weight (MW), X-ray density (d_x), Bulk density (d_B), and Porosity (P %), of $Mg_{1-x}Zn_xFe_2O_4$ system (x=0.00 and 0.30).

Comp. 'x'	a (Å)	V ($Å^3$)	MW (gm/mol)	d_x (gm/cm^3)	d_B (gm/cm^3)	P (%)
0.00	8.341	580.3	199.9	4.57	3.82	17
0.30	8.352	582.6	208.2	4.74	3.85	19

Magnetization:

The magnetic properties of $Mg_{1-x}Zn_xFe_2O_4$ (x = 0.00 and 0.30) studied by using pulse field hysteresis loop tracer technique at room temperature. The M-H plots of both the samples are presented in figure 2.

It is observed from the M-H plots that both samples exhibit the ferromagnetic nature. The magnetic parameters such as saturation magnetization, remanence magnetization and coercivity were obtained by the M-H plots and tabulated in table 4. It is observed from table 4 that the saturation magnetization found to increase on substitution of zinc, while the coercivity decreases from 85Oe to 41Oe. It also observed that the remanence magnetization increases with zinc which can be attributed to the increase of saturation magnetization. The observed results are similar to that of Zn-Mg spinel ferrite nanoparticles prepared by co-precipitation [18]. The observed behavior of the magnetization can be explained on the basis of Neel's model of ferrimagnetism. It is well known that the Zn^{2+} have the strong preference to tetrahedral site, Mg^{2+} occupy octahedral [B] site and Fe^{3+} can occupy both tetrahedral (A) and octahedral [B] sites. When zinc ions substituted they occupy tetrahedral (A) site by displacing the Fe^{3+} ions to octahedral [B] site. This migration strengthens the A-B exchange interaction which results in the

increase in the net magnetization. Thus, saturation magnetization increases with zinc substitution.

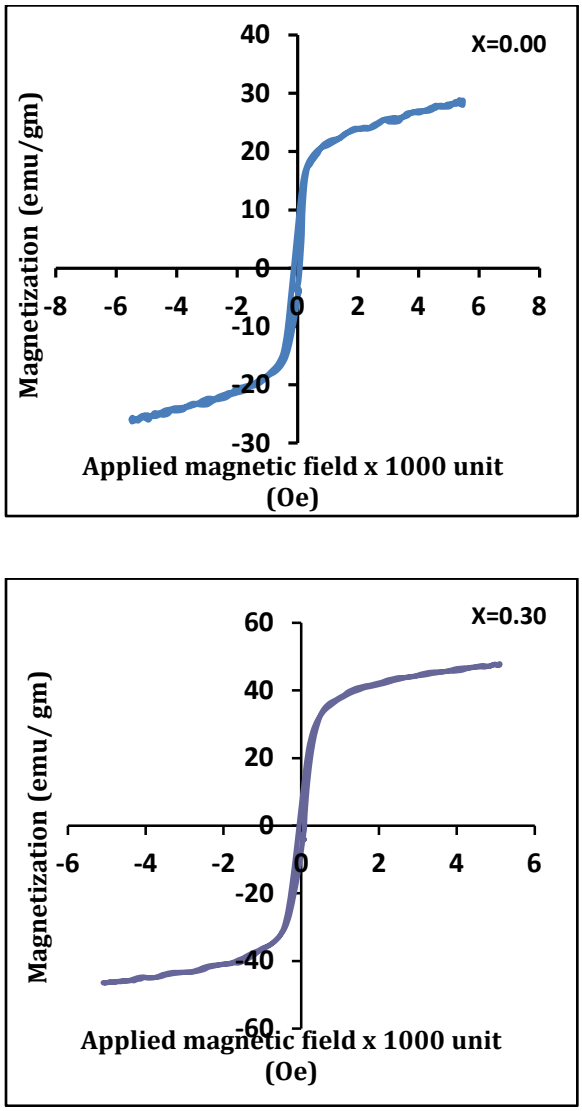

Figure 2: M-H plots of $Mg_{1-x}Zn_xFe_2O_4$ (x = 0.00 and 0.30)

Table 4: Saturation magnetization (M_s), Remanence magnetization (M_r), Coercivity (H_c) of $Mg_{1-x}Zn_xFe_2O_4$ system (x=0.00 and 0.30).

Comp. 'x'	Ms (emu/gm)	Mr (emu/gm)	Hc (Oe)
0.00	28.83	0.16	84.98
0.30	40.01	1.07	40.83

Conclusion:

The XRD patterns revealed the single phase cubic spinel structure of prepared Mg-Zn spinel ferrite nanoparticles. The obtained structural parameters are in the reported range. The ferromagnetic behaviour of the bare and zinc substituted magnesium spinel ferrite nanoparticles was exhibited. The enhancement in saturation magnetization was observed on zinc substitution.

Acknowledgement:

The Author is very much thankful to Dr. K. M. Jadhav, Professor, department of physics, Dr. Babasaheb Ambedkar Marathwada University, Aurangabad for magnetic measurements and discussions

References:

[1]. J. Smit,, H.P.J. Wijin, Ferrites, Philips Technical Library, 1959.
[2]. S.E. Shirsath, B.G. Toksha, M.L. Mane, V.N. Dhage, D.R. Shengule, K.M. Jadhav, Powder Technol. 212 (2011) 218.
[3]. M.L. Mane, V.N. Dhage, R. Sundar, K. Ranganathan, S.M. Oak, D.R. Shengule, K.M. Jadhav, Appl. Surf. Sci. 257 (2011) 8511.
[4]. M.A. Ahmed, Samiha T. Bishay, S.I. El-dek, G. Omar, J. Alloys Compd. 509 (2011) 805.
[5]. X. Hou, J. Feng, X. Liu, Y. Ren, Z. Fan, M. Zhang, J. Colloid Interface Sci. 353 (2011) 524.
[6]. C. Venkatarajua, G. Sathishkumar, K. Sivakumar, J. Alloys Compd. 498 (2010) 203.
[7]. S.C. Watawe, U.A. Bamne, S.P. Gonbare, R.B. Tangsali, Mater. Chem. Phys. 103 (2007) 323.
[8]. V. Šepelak, D.Baabe, D.Mienert, F.J.Litterst, K.D.Becker, Scr. Mater. 48 (2003) 961.
[9]. Y. Ichiyanagi, M.Kubota, S.Moritake, Y.Kanazawa, T.Yamada, T. Uehashi, J. Magn. Magn. Mater. 310 (2007) 2378.
[10]. K.P. Thummer,M.C.Chhantbar,K.B.Modi,G.J.Baldha,H.H.Joshi,J. Magn. Magn. Mater. 280 (2004) 23–30.
[11]. R.G. Kulkarni, H.H.Joshi, Solid State Commun.53 (1985) 1005–1008.
[12]. A. Manikandan, J.J.Vijaya, M.Sundararajan, C. Meganathan, L.J. Kennedy, M. Bououdina, Superlattice Microstruct. 64 (2013) 118–131.
[13]. G. Chandrasekaran, P.N.Sebastian, Mater. Lett. 37 (1998) 17.
[14]. M.A. Ahmed, E.Ateia, S.I.El-Dek, Mater. Lett. 57 (2003) 4256–4266.
[15]. D. Ravinder, L.Balachander, Y.C.Venudhar, Mater. Lett. 49 (2001) 267–271.

[16]. V. R. Bhagwat, Shankar. D. Birajdar, Ashok V.Humbe, Pankaj P. Khirade, K. M. Jadhav, International Journal of Advanced Research in Basic and Applied Science, vol 2, (2015) 5-8
[17]. R. C. Alange, et. al. International Journal of Advanced Research in Basic and Applied Science, vol 2, (2016) 33-35
[18]. K. Nadeemn, S.Rahman,M.Mumtaz, Progress in Natural Science: Materials International 25 (2015) 111–116